THE ASTROPHYSICAL JOURNAL, 502:L33–L37, 1998 July 20

MICROLENSING BY MULTIPLE PLANETS IN HIGH-MAGNIFICATION EVENTS

B. SCOTT GAUDI
Ohio State University, Department of Astronomy, 5040 Smith Laboratory, 174 West 18th Avenue, Columbus, OH 43210;
gaudi@astronomy.ohio-state.edu
AND
RICHARD M. NABER AND PENNY D. SACKETT
Kapteyn Astronomical Institute, Postbus 800, 9700 AV Groningen, The Netherlands; richard@astro.rug.nl, psackett@astro.rug.nl
Received 1998 March 25; accepted 1998 May 21; published 1998 July 1

ABSTRACT

Microlensing is increasingly gaining recognition as a powerful method for the detection and characterization of extrasolar planetary systems. Naively, one might expect that the probability of detecting the influence of more than one planet on any single microlensing light curve would be small. Recently, however, Griest & Safizadeh have shown that, for a subset of events, those with minimum-impact parameter $u_{\rm min} \lesssim 0.1$ (high-magnification events), the detection probability is nearly 100% for Jovian-mass planets with projected separations in the range 0.6–1.6 of the primary Einstein ring radius $R_{\rm E}$ and remains substantial outside this zone. In this Letter, we point out that this result implies that, regardless of orientation, *all* Jovian-mass planets with separations near 0.6–1.6$R_{\rm E}$ dramatically affect the central region of the magnification pattern and thus have a significant probability of being detected (or ruled out) in high-magnification events. The joint probability, averaged over all inclinations and phases, of two planets having projected separations within 0.6–1.6$R_{\rm E}$ is substantial: 1%–15% for two planets with the intrinsic separations of Jupiter and Saturn orbiting around 0.3–1.0 $M_\odot$ parent stars. We illustrate by example the complicated magnification patterns and light curves that can result when two planets are present, and we discuss the possible implications of our result on detection efficiencies and the ability to discriminate between multiple and single planets in high-magnification events.

Subject headings: gravitational lensing — planetary systems

1. INTRODUCTION

A planetary microlensing event occurs whenever the presence of a planet creates a perturbation to the standard microlensing event light curve. These perturbations typically have magnitudes of $\lesssim$20% and durations of a few days or less. First suggested by Mao & Paczyński (1991) as a method to detect extrasolar planetary systems, the possibility was explored further by Gould & Loeb (1992), who found that roughly 15% of microlensing light curves should show evidence of planetary deviations if all primary lenses have Jupiter-mass planets with orbital separations comparable to that of Jupiter. Although these probabilities are relatively high, the use of microlensing to discover planets was largely ignored since in searching for primary events the microlensing survey teams must monitor millions of stars in very crowded fields, resulting in temporal sampling that is too low (~1 day) and photometric errors that are too high ($\gtrsim$5%) to detect most secondary planetary deviations (Alcock et al. 1997a).

Recently the situation has changed dramatically as the real-time data reduction of the survey teams has enabled them to issue electronic "alerts," which are notifications of ongoing events detected before the peak magnification (Udalski et al. 1994; Pratt et al. 1996). Over 60 events are currently alerted per year toward the Galactic bulge. Only a handful of these are ongoing at any given time; this has allowed the PLANET (Albrow et al. 1997, 1998) and GMAN (Pratt et al. 1996; Alcock et al. 1997b) collaborations to sample events very densely and with high photometric accuracy, enabling—in principle—the detection of planetary anomalies. No clear planetary detections have yet been made in this way, but preliminary estimates of detection efficiencies show that PLANET, over the next two observing seasons, should be sensitive to planetary anomalies caused by Jovian planets orbiting a few astronomical units from their parent stars (Albrow et al. 1998). Thus, if these kinds of planets are common, they should be detected soon. If not, microlensing will be able to place interesting upper limits on the frequency of such systems.

These observational developments have been accompanied by an explosion of theoretical work, including further studies of detection probabilities and observing strategies that incorporate a variety of new effects (Bolatto & Falco 1994; Bennett & Rhie 1996; Peale 1997; Sackett 1997; Di Stefano & Scalzo 1998a, 1998b), the demonstration of planetary microlensing light curves (Wambsganss 1997), explorations of the degeneracies in the fits of planetary events (Gaudi & Gould 1997; Gaudi 1998), and a study of the relation between binary and planetary lenses (Dominik 1998). It would thus seem that the theoretical understanding of the detection and characterization of planetary systems using microlensing should be well in hand.

However, the field still has surprises to offer. Recently, Griest & Safizadeh (1998, hereafter GS) came to a rather startling conclusion: for microlensing events with minimum-impact parameter $u_{\rm min} \lesssim 0.1$ (maximum magnification $A \gtrsim 10$), the detection probability is nearly 100% for Jovian-mass planets with projected separations lying within 0.6–1.6 of the Einstein ring of the primary, i.e., the so-called "standard lensing zone." In fact, GS found that the detection probability for this subset of events is higher for *all* projected separations and preferentially so for smaller separations. Since the probability that an event will have impact parameter $u_{\rm min} < 0.1$ is ~10%, this means that, for ~10% of all events, the existence of a planet in the lensing zone can be detected or ruled out. The primary point of this Letter is to stress that the conclusions of GS necessarily imply that, regardless of orientation, *all* Jovian-mass planets in the lensing zone dramatically affect the central region of the magnification pattern and thus have a significant probability of

being detected (or ruled out) in small-impact parameter (high-magnification) events.

We present here a preliminary exploration of microlensing by lenses orbited by multiple (two) planets. In order to assess the frequency with which multiple planets may lie at detectable separations, we calculate in § 2 the probability of two planets having projected separations in the standard lensing zone, and then indicate why an even larger zone is more appropriate for high-magnification events. In § 3, we briefly review the formalism needed for calculating the magnification patterns created by single, double, and triple lenses, and in § 4, we present sample light curves. In § 5, we discuss the possible implications of our results and conclude.

2. "LENSING ZONE" FREQUENCIES FOR MULTIPLE PLANETS

The "standard lensing zone" is generally defined as the annular region in the source plane with $0.6 \leq r \leq 1.6R_{\rm E}$, where $R_{\rm E}$ is the Einstein ring of the parent star,

$$R_{\rm E} = \left[\frac{4GMD_{\rm OL}\,(1 - D_{\rm OL}/D_{\rm OS})}{c^2}\right]^{1/2} = 3.5\ {\rm AU}\left(\frac{M}{M_\odot}\right)^{1/2}, \quad (2.1)$$

and M is the mass of the primary lens. For the scaling relation on the far right-hand side, we have assumed a source distance $D_{\rm OS} = 8$ kpc and a lens distance $D_{\rm OL} = 6$ kpc. With these assumed distances, the lensing zone corresponds to 2.1–5.6 AU for a 1.0 $M_\odot$ primary and 1.1–3.0 AU for a 0.3 $M_\odot$ primary.

The standard lensing zone corresponds to the range of projected separations $b \equiv r/R_{\rm E}$ for which planets will have substantial detection probabilities, averaging over all possible impact parameters ($0 \leq u_{\rm min} \lesssim 1$). For high-magnification events ($A > 10$), however, GS have shown that the planets with a mass ratio $q \gtrsim 0.001$ may be detected with nearly 100% probability, even when they lie somewhat outside the lensing zone. This is true because in high-magnification events the planetary anomaly is caused by the source approaching or crossing the central caustic, which is always near the primary, regardless of orientation and separation. In contrast, for low-magnification events, the source must approach the planetary caustic, whose position depends on the projected separation of the planet, and whose detectability depends on the orientation of the trajectory. The results of GS in turn imply that *multiple planets* in the lensing zone will also create significant perturbations in high-magnification events, providing such a scenario occurs frequently enough.

Given two planets with true separations (in units of $R_{\rm E}$) of a_1 and a_2, we thus wish to calculate the joint probability that the projected separations b_1 and b_2 will fall in the lensing zone. The relation between the true and projected separations is $b_k = a_k\,(\cos^2\phi_k + \sin^2\phi_k \cos^2 i)^{1/2}$, where i is the orbital inclination and ϕ_k is the orbital phase of planet k, and we have assumed circular, coplanar orbits. The calculation of the probability involves a three-dimensional integral over $\cos i$, ϕ_1, and ϕ_2, the distributions of which are flat. The result is shown in Figure 1 as a function of a_2, for several discrete values of a_1 representing known or plausible planetary systems with Jovian-mass planets. The separations in physical units (astronomical units) scale according to equation (2.1).

It is apparent from Figure 1 that the joint probability of two

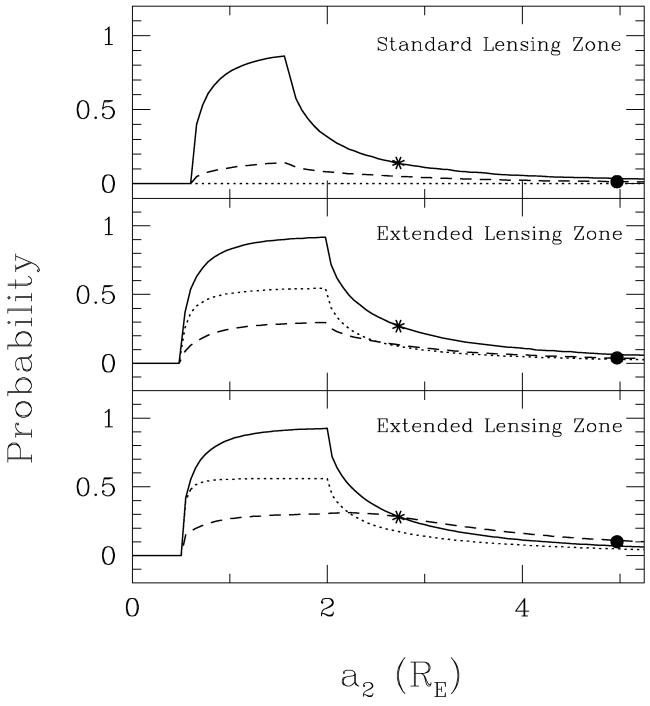

FIG. 1.—*Upper panel*: the joint probability that two planets with true separations a_1 and a_2 (in units of the Einstein ring radius $R_{\rm E}$ of the system) will have projected separations, b_1 and b_2, lying in the standard lensing zone, defined as $0.6 < b < 1.6$. The probability is shown as a function of a_2, for $a_1 = 1.5$ (*solid line*, appropriate to Jupiter orbiting a 1.0 $M_\odot$ primary), $a_1 = 0.6$ (*dotted line*, appropriate to 47 UMa), and $a_1 = 2.7$ (*dashed line*, appropriate to Jupiter orbiting a 0.3 $M_\odot$ primary). The probability for two planets with true separations of Jupiter and Saturn are indicated for a solar-mass primary (*asterisk*) and a 0.3 $M_\odot$ primary (*filled circle*). *Middle panel*: same as upper panel, but for the extended lensing zone, $0.5 < b < 2.0$. *Lower panel*: the conditional probability that both b_1 and b_2 have projected separations in the extended lensing zone, given that either b_1 or b_2 satisfies this criterion.

Jovian planets falling in the lensing zone, regardless of their relative positions, may be quite high. Note, in particular, the long tail for higher true separations a_2. Furthermore, the *conditional* probability (lower panel of Fig. 1), i.e., the probability that both planets will be in the lensing zone given that one of the planets already meets this criterion, is even higher. For high-magnification events, this implies that it is highly probable that if deviations from one planet are present, deviations from the second planet are present as well. For planets with true separations equal to that of Jupiter and Saturn (5.2 and 9.5 AU, respectively), the probability of both planets being in the lensing zone is 14% if the planets are orbiting a 1.0 $M_\odot$ primary, and 1% for a 0.3 $M_\odot$ primary.

Radial velocity techniques have discovered several Jovian-mass planets, many with orbital separations substantially smaller than 1 AU (Mayor & Queloz 1995; Butler & Marcy 1996), making them difficult to detect via microlensing. Other planets detected by radial velocity methods, like the 3 M_J planet orbiting the G0 star 47 UMa on a circular orbit at 2.1 AU, would be detectable in high-magnification events, especially if in combination with other planets. As the upper panel of Figure 1 shows, the planet orbiting 47 UMa would never fall in the standard lensing zone of a 1.0 $M_\odot$ primary but would have a substantial probability ($\gtrsim$10%) of falling with a slightly extended zone defined by 0.5–2.0$R_{\rm E}$ (middle panel of Fig. 1) simultaneously with other planets orbiting over a wide range.

This distinction is important since, as GS have shown, the probability of Jovian-mass detection in high-magnification events remains high even in this more expanded lensing zone.

The frequency with which multiple planets will reveal themselves in high-amplification events depends on their actual frequency and the distribution of their orbital radius and mass. Let us consider the familiar system of a Jupiter and Saturn orbiting a 1.0 $M_\odot$ primary. Convolving the detection efficiencies of GS as a function of projected separation b with the likelihood that Jupiter would have that b simultaneously with Saturn falling in the extended 0.5–2.0R_E lensing zone, we find that ~12% of events with $u_{min} < 0.1$ would reveal the existence of the multiple planets. If 100 events were alerted per year, then intense monitoring of the ~10 events with $u_{min} < 0.1$ could be expected to yield about one multiple-planet lensing event per year, if all Galactic lenses have planetary systems like our own solar system.

3. SINGLE, DOUBLE, AND TRIPLE LENSES

In this section, we briefly review and apply the formalism needed for calculating the magnification that results from single, double, and triple lens configurations. Let us consider a source with projected position (ξ, η). Following Witt (1990), we write this in complex coordinates as $\zeta = \xi + i\eta$. Lensing is the mapping from the source position ζ to the image positions $z = x + iy$ given by the lens equation, which, for N-point masses, is (Witt 1990)

$$\zeta = z + \sum_k^N \frac{\epsilon_k}{\overline{z_k} - \overline{z}}, \tag{3.1}$$

where z_k is the (complex) coordinate of mass k, ϵ_k is the fractional mass of lens component k, and all distances are in units of the angular Einstein ring, $\theta_E \equiv R_E/D_{OL}$. The magnification A_j of each image j is given by the determinant of the Jacobian of the mapping in equation (3.1), evaluated at that image position,

$$A_j = \frac{1}{|\det J|}\Bigg|_{z=z_j}, \quad \det J = 1 - \frac{\partial\zeta}{\partial\overline{z}}\frac{\overline{\partial\zeta}}{\partial\overline{z}} \tag{3.2}$$

In microlensing, the images are unresolved, and the total magnification is given by the sum of the individual magnifications, $A = \sum_j A_j$. The set of source positions for which the magnification is formally infinite, given by the condition $\det J = 0$, defines a set of closed curves called caustics. We will label the most massive (or only) component of the lens as 1 and define the origin as $z_1 = 0$.

For the single lens ($N = 1$) case, the positions and magnifications of the two resulting images can be found analytically, and their total magnification is

$$A_0 = \frac{u^2 + 2}{u\,(u^2 + 4)^{1/2}}, \tag{3.3}$$

where $u \equiv |\zeta|$. For $u \to 0$, $A_0 \to \infty$, and the point $u = 0$ defines the caustic in the single-lens case. For rectilinear motion, $u = [(t - t_0)^2/t_E^2 + u_{min}^2]^{1/2}$, where t_0 is the time of maximum magnification, u_{min} is the minimum-impact parameter, and t_E is the timescale of the event defined as $t_E = R_E/v_\perp$, and $v_\perp$ is the transverse velocity of the lens relative to the observer-source line of sight. A single-lens light curve is then given by $F = A_0F_0$, where F_0 is the unlensed flux of the source, and is a function of four parameters: t_0, t_E, u_{min}, and F_0.

For a double lens ($N = 2$), equation (3.1) is equivalent to a fifth-order complex polynomial in z. The solution yields three or five images, with the number of images changing by two as the source crosses a caustic. A binary lens generates one, two, or three caustic curves, in all cases separate and nonintersecting. The light curve of a binary lens is a function of seven parameters: the four parameters describing the single-lens case, the additional parameters b, the separation of the lenses in units of θ_E, q, the mass ratio of the system, and θ, the angle of the source trajectory with respect to the binary axis.

Adding a third component to the lens system increases the complexity enormously; in particular, the caustics can exhibit self-intersection and nesting. Equation (3.1) is now equivalent to a (rather cumbersome) 10th-order polynomial in z. There are thus a maximum of 10 images and a minimum of four images, with the number of images changing by a multiple of 2 (Rhie 1997) as the source crosses a caustic. Rather than directly solving the 10th-order equation, we adopt the alternate approach of inverse-ray shooting (see Wambsganss 1997 and references therein). A triple-lens light curve is a function of 10 parameters: the four single-lens parameters, the separations and mass ratios b_1, b_2 and q_1, q_2, the angle of the source trajectory θ, and $\Delta\theta$, the angle between the position vectors of the two companions.

For binary and triple systems with small mass ratio(s), most source positions have magnifications that are nearly identical to that of a single lens, A_0. It is thus useful to define the fractional deviation, $\delta \equiv (A - A_0)/A_0$, where A is the true (binary- or ternary-lens) magnification.

4. ILLUSTRATING THE EFFECT OF MULTIPLE PLANETS

An exhaustive study of triple lenses, which would necessitate an exploration of the q_1, q_2, b_1, b_2, and $\Delta\theta$ parameter space, is quite beyond the scope of this Letter. However, in order to illustrate the effect that a third lens would have on typical light curves, we consider Jovian planets orbiting stars that are common in the Galaxy. Fixing $b_1 = 1.2$ and $q_1 = 0.003$, corresponding to a Jovian-mass planet orbiting a 0.3 $M_\odot$ primary, or a 3 M_J planet orbiting a solar-mass primary, we vary the b_2 of the second planet with a mass ratio $q_2 = 0.001$, corresponding to a Saturn-mass planet (0.3 $M_\odot$ primary) or a Jupiter-mass planet (1.0 $M_\odot$ primary). We concentrate on only those source positions $|\zeta| \leq 0.1$ for which the planets have a significant cooperative effect. The left panels of Figure 2 show the magnification pattern for several separations b_2 and relative angles $\Delta\theta$. For comparison, we also show the magnification pattern when only the planet with a mass ratio $q_1 = 0.003$ is present. For these maps, we have adopted a uniformly bright source with a radius appropriate to a main-sequence star, $\rho = \theta_*/\theta_E \simeq 0.003\,(R_*/R_\odot)$, where θ_* and R_* are the angular and physical sizes of the source, respectively, and we have assumed $D_{OL} = 6$ kpc, $D_{OS} = 8$ kpc, and $M = 0.3\ M_\odot$.

Note that the case with $b_2 = 1.2$ and $\Delta\theta = 0$ is completely degenerate with those from a single planet with a mass ratio $q = q_1 + q_2 = 0.004$. Although for other configurations the magnification patterns with and without the second planet appear dramatically different, it should be kept in mind that what

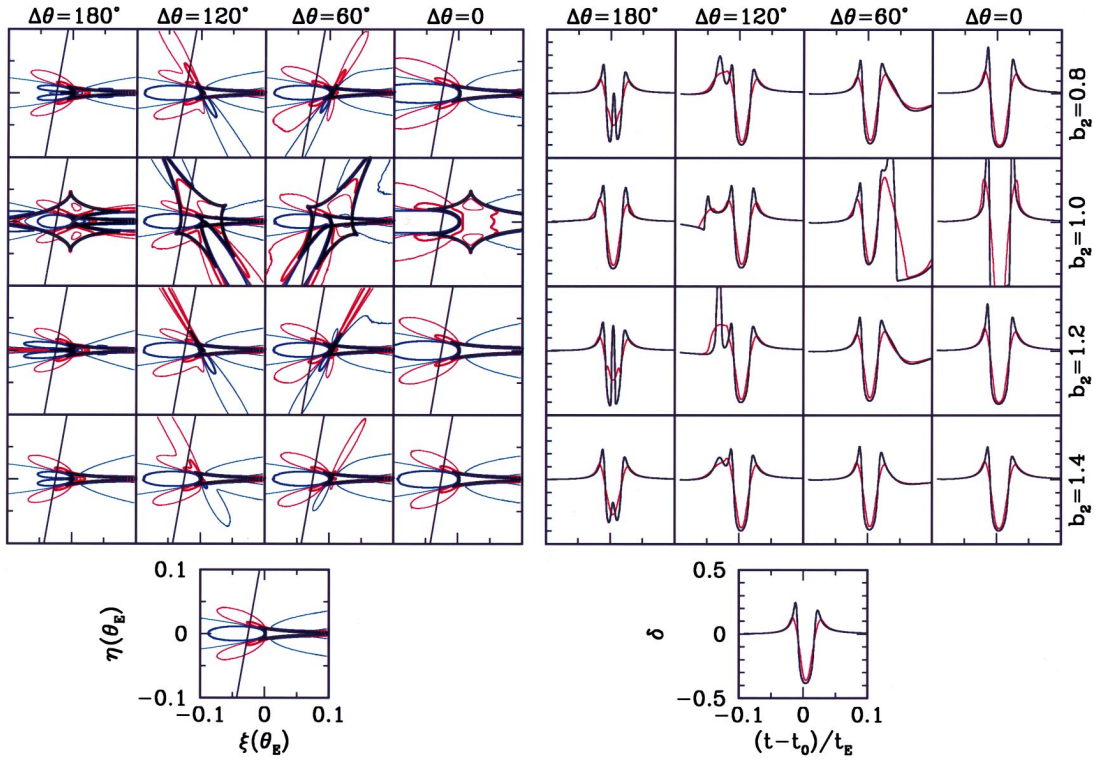

FIG. 2.—*Left panels*: contours of constant fractional deviation δ from the single-mass lens magnification, as a function of source position (ξ, η) in units of the angular Einstein ring, θ_E. The parameters of planet 1 are held fixed at $q_1 = 0.003$, $b_1 = 1.2$, while the projected separation b_2 and the angle between the axes, $\Delta\theta$, are varied for a second planet with $q_2 = 0.001$. The offset panel is the case when only planet 1 is present. The contours are $\delta = \pm 5\%$ (*light lines*) and $\pm 20\%$ (*bold lines*). Positive contours are red, negative contours are blue. The caustics ($\delta = \infty$) are shown in black. A trajectory with minimum-impact parameter $u_{min} = 0.025$ and angle $\theta = 260^\circ$ with respect to axis 1 is shown. The scales on the axes are the same for all panels. *Right panels*: the fractional deviation δ from a single-mass lens as a function of time for the trajectories shown in the left panels. The black line is for a source of radius $\rho = 0.003$ in units of θ_E; the red line is for $\rho = 0.01$. The scale of all the axes is the same for all panels.

one actually measures are light curves, which are one-dimensional cuts through these diagrams. Light curves are shown in the right panels of Figure 2, with source radii of $\rho = 0.003$ and $\rho = 0.01$, for the sample-source trajectory indicated in the left panels. Some geometries give rise to light curves that deviate dramatically from the case with only one planet, but those with $\Delta\theta = 0$ have shapes that are very similar to single-planet lensing, although with larger amplitude and duration. In other words, some two-planet geometries with $\Delta\theta \sim 0$ will give rise to light curves that are degenerate with single planets of larger mass ratios. Furthermore, note that regions of positive and negative deviations are more closely spaced when two planets are present. When finite-source effects are considered, the overall amplitude of the multiple-planet anomaly will thus be suppressed. Examples can be seen in the $b_2 = 1.2$ and 0.8 and $\Delta\theta = 180^\circ$ panels of Figure 2, where, for source radius $\rho = 0.01$, the amplitude of the anomaly is smaller for the double planetary system than the single-planet system, while for $\rho = 0.003$, the amplitudes are similar. Overall detection probabilities may thus be lower for high-magnification events when multiple planets and large sources are considered.

5. IMPLICATIONS AND CONCLUSION

In this Letter, we have demonstrated that (1) the probability of two planets having projected separations that fall in the "standard lensing zone" ($0.6 < b < 1.6$) is quite high, ~1%–15% for planets with true separations corresponding to Jupiter and Saturn orbiting stars of typical mass; (2) the influence of multiple planets in and somewhat beyond the standard lensing zone can be profound for high-magnification events ($u_{min} < 0.1$); however, (3) for some geometries, the magnification pattern and resulting light curves from multiple planets are qualitatively degenerate with those from single-planet lensing; and (4) for high-magnification events, finite-source effects are likely to suppress more substantially the amplitude of multiple-planet deviations than the amplitude of single-planet deviations.

Given these results, it would appear that the effects of multiple planets warrant future study. All previous theoretical studies have calculated microlensing planet-detection sensitivities either by ignoring multiple planets or by treating each planet independently. For high-impact parameter events (low magnification), this is probably a fair assumption, but as the magnification maps in Figure 2 illustrate, detection probabilities will need to be revised for small-impact parameters (large magnification). The sense of revision will likely depend on finite-source effects. It is also likely that for some geometries, serious degeneracies exist between light curves arising from multiple- and single-planet high-magnification events; these degeneracies are above and beyond those present in the single-planet case discussed by GS. This possible degeneracy is especially pertinent in light of the fact that the conditional probability of having two planets in the lensing zone is substantial. Thus, the interpretation of any given high-magnification event may be difficult: the degeneracies should be characterized and their severity determined in order to have a clear understanding of the kinds of systems whose parameters can be unambiguously determined from the deviations. Finally, the calculation of

planet-detection efficiencies for high-magnification events should consider multiple planets in order to be able to convert reliably the observed frequency of planetary deviations into a true frequency of planetary systems.

We would like to thank the members of the PLANET collaboration, and especially Martin Dominik, for comments on an earlier version of this Letter. This work was supported by grant AST-95-3061 from the NSF, the Kapteyn Astronomical Institute, and NWO grant 781-76-018.

REFERENCES

Albrow, M., et al. 1997, in Variable Stars and the Astrophysical Returns of Microlensing Surveys, ed. R. Ferlet, J.-P. Maillard, & B. Raban (Gif-sur-Yvette: Editions Frontières), 135
———. 1998, ApJ, submitted
Alcock, C., et al. 1997a, ApJ, 479, 119
———. 1997b, ApJ, 491, 436
Bennett, D., & Rhie, S. H. 1996, ApJ, 472, 660
Bolatto, A. D., & Falco, E. E. 1994, ApJ, 436, 112
Butler, P., & Marcy, G. 1996, ApJ, 464, L15
Di Stefano, R., & Scalzo, R. 1998a, ApJ, submitted
———. 1998b, ApJ, submitted
Dominik, M. 1998, in preparation
Gaudi, B. S. 1998, ApJ, in press
Gaudi, B. S., & Gould, A. 1997, ApJ, 486, 85
Gould, A., & Loeb, A. 1992, ApJ, 396, 104
Griest, K., & Safizadeh, N. 1998, ApJ, 500, 37 (GS)
Mao, S., & Paczyński, B. 1991, ApJ, 374, 37
Mayor, M., & Queloz, D. 1995, Nature, 378, 355
Peale, S. J. 1997, Icarus, 127, 269
Pratt, M. R., et al. 1996, in IAU Symp. 173, Astrophysical Applications of Gravitational Microlensing, ed. C. S. Kochanek & J. N. Hewitt (Dordrecht: Kluwer), 221
Rhie, S. H. 1997, ApJ, 484, 63
Sackett, P. D. 1997, in Final Rep. ESO Working Group on Detection of Extrasolar Planets, ed. F. Paresce & A. Renzini (Garching: ESO), C1–C21
Udalski, A., et al. 1994, Acta Astron., 44, 227
Wambsganss, J. 1997, MNRAS, 284, 172
Witt, H. 1990, A&A, 236, 311